Orthogonal Time Frequency Space Modulation in Multiple-Antenna Systems

WANG Dong[1], WANG Fanggang[1], LI Xiran[1], YUAN Pu[2], JIANG Dajie[2]

(1. State Key Laboratory of Rail Traffic Control and Safety, Beijing Jiaotong University, Beijing 100044, China;
2. Vivo Mobile Communication Co., Ltd., Beijing 100016, China)

Abstract: The application of the orthogonal time frequency space (OTFS) modulation in multiple-antenna systems is investigated. The diversity and/or the multiplexing gain can be achieved by deploying various multiple-antenna techniques, and thus the reliability and/or the spectral efficiency are improved correspondingly. We provide two classes of OTFS-based multiple-antenna approaches for both the open-loop and the closed-loop systems. Specifically, in the open-loop system, a transmitting diversity approach, which resembles the space-time coding technique, is proposed by allocating the information symbols appropriately in the delay-Doppler domain. In the closed-loop system, we adopt the Tomlinson-Harashima precoding in our derived delay-Doppler equivalent transmission model. Numerical evaluations demonstrate the advantages of applying the multiple-antenna techniques to the OTFS. At last, several challenges and opportunities are presented.

Keywords: OTFS; space-time coding; Tomlinson-Harashima precoding

DOI: 10.12142/ZTECOM.202104008

https://kns.cnki.net/kcms/detail/34.1294.TN.20211102.1456.002.html, published online December 5, 2021

Manuscript received: 2021-10-13

Citation (IEEE Format): D. Wang, F. G. Wang, X. R. Li, et al., "Orthogonal time frequency space modulation in multiple-antenna systems," *ZTE Communications*, vol. 19, no. 4, pp. 71–78, Dec. 2021. doi: 10.12142/ZTECOM.202104008.

1 Introduction

Recently, the orthogonal time frequency space (OTFS) modulation has been proposed to deal with the severe inter-carrier interference problem caused by the Doppler effect in the high-speed mobility scenario[1]. In the OTFS system, the modulation symbols are multiplexed in the delay-Doppler domain instead of the time-frequency domain, which provides an alternative representation of a time-varying channel geometry modeling of the transmission paths[2]. However, the two-dimensional convolution of the input-output relation in the OTFS system makes the equalization involved. The OTFS equalization schemes have been extensively studied[3–5]. In Ref. [3], a message-passing (MP) algorithm was developed for joint interference cancellation and symbol detection. In Ref. [4], the authors proposed a cross domain iterative detection algorithm to enhance the error performance of OTFS modulation.

By utilizing the mathematical least-square minimum residual algorithm, the authors in Ref. [5] proposed a low-complexity equalizer and a block-wise interference eliminator.

The aforementioned OTFS schemes focus on the single-input and single-output system. By exploiting the multiple antenna techniques, the reliability and/or the spectral efficiency can be improved in the OTFS multiple-antenna system. Similar to the orthogonal frequency division multiplexing (OFDM) multiple-antenna system, the transmission schemes in the OTFS multiple-antenna system can be categorized into two classes: open-loop and closed-loop. The main difference is that the channel state information (CSI) reported to the transmitter is

This work was supported in part by the Fundamental Research Funds for the Central Universities under Grant Nos. 2020JBM081 and 2020JBZD005, in part by the National Key R&D Program of China under Grant 2020YFB1806903, in part by the National Natural Science Foundation under Grant No. U1834210.

required in the closed-loop system whereas it is not necessary for the open-loop system. In the literature of the open-loop OTFS, the authors in Ref. [6] proposed a low-complexity linear equalizer by utilizing the block circulant property of the equivalent channel. In Ref. [7], the quasi-banded sparse structure of the equalization matrix was used to design a low-complexity linear equalization scheme in the delay-Doppler domain. However, the transmission schemes in Refs. [6] and [7] only consider the equalization at the receiver without designing the transmitter, the spatial diversity of which is not fully exploited. Then, several papers studied the spatial diversity schemes in OTFS multiple-antenna systems, which can be harnessed by the space-time coding scheme[8 – 10]. In Ref. [11], a space-time coding scheme with cyclic delay diversity was presented. By assuming that the delay-Doppler channel is invariant in the two consecutive OTFS frames, a space-time code using the Alamouti code structure is proposed in the open-loop system[12]. However, the channel varies drastically in the two consecutive OTFS frames under the high-speed scenarios, which degrades the bit error ratio (BER) performance. In the closed-loop transmission, the feedback of the channel information is required, which further improves the throughput of the OTFS multiple-antenna system. The authors in Ref. [13] proposed a Tomlinson-Harashima precoding (THP) scheme in the delay-time domain. In Ref. [14], an uplink-aided high mobility downlink channel estimation scheme for the massive multiple-input and multiple-output (MIMO) -OTFS systems was proposed. The expectation-maximization-based variational Bayesian framework was adopted to recover the uplink channel parameters including the angle, the delay, the Doppler frequency, and the channel gain for each physical scattering path. Then, in Ref. [15], the authors designed an effective path scheduling algorithm to map different users to the delay-Doppler domain grids without inter-user interference in the same OTFS block. The authors in Ref. [16] proposed a maximal ratio combining (MRC) precoding scheme in the multi-user massive MIMO-OTFS system. However, the previous work mainly focuses on the ideal pulse shaping for the transmission design whereas the problem of its application with the practical pulses, such as the rectangular pulse shaping, is not fully addressed.

In this paper, we investigate the transmission schemes in the open-loop and closed-loop OTFS multiple-antenna systems. We preclude the assumption that the channel states in the two consecutive frames are invariant. Both the ideal pulse shaping and the rectangular pulse shaping are studied. The main contributions of this paper are summarized as follows:

• We design a transmit diversity approach within one OTFS frame duration in the open-loop systems. The guards are carefully allocated to avoid sub-frames interfering with each other and to ensure the two sub-frames can be regarded as passing the identical channel in the delay-Doppler domain.

• We then design a scheme with the rectangular pulse shaping. In addition to the guards in the ideal pulse shaping, we place the guards at the last l_{max} symbols along the delay domain in the rectangular pulse shaping. Then, the channel of each sub-frame in the equivalent transmission model is identical.

• We further indicate that the linear precoding in the time-frequency domain can be alternatively expressed in the delay-Doppler domain. By deriving the equivalent transmission model in the OTFS system, the THP-based schemes in the delay-Doppler domain under the zero-forcing (ZF) and minimum mean square error (MMSE) criterion are designed.

2 Open-Loop System

In the open-loop system, the channel information is not required at the transmitter, which is suitable for the transmission in the high-speed scenarios. In contrast to the two-frame block fading assumption[12], we introduce the transmit diversity approach within one OTFS frame duration by appropriately allocating information symbols, guards, and pilots with the ideal pulse shaping and rectangular pulse shaping.

2.1 Spatial Diversity Approach

In this paper, we consider the wide-sense non-stationary channel with the Jakes' formula, different from the wide-sense stationary channel. The amplitude and the phase shift of each path are different in the two consecutive frames, which causes the delay-Doppler channel changes. The traditional space-time coding is applied on two-time slots by assuming the invariant channel, which is not practical in the non-stationary channel. Then, how to design a transmit diversity within one frame duration is a challenge in the OTFS system. Considering a scenario that the transmitter is equipped with two antennas and the receiver is equipped with a single antenna, we propose a spatial diversity scheme within one frame by allocating information symbols, guards, and pilots. The positions of information symbols and guards are the same for each transmit antenna, which is shown in Fig. 1. Information symbols, guards, and pilots are appropriately allocated in one OTFS frame. In addition to the guards allocated in the ideal pulse shaping, we place the guards at the last l_{max} symbols along the delay domain in the rectangular pulse shaping. Then, the channel of each sub-frame in the equivalent transmission model is identical.

Firstly, we divide the resource units of a frame into two sub-frames along the Doppler domain. Symbols in the first sub-frame and the second sub-frame are expressed as $x[l,k_1], k_1 \in \{0,1,...,\frac{N}{2}-1\}$ and $x[l,k_2], k_2 \in \{\frac{N}{2},\frac{N}{2}+1,...,N-1\}$, respectively. Then, the received signal of each sub-frame can be obtained as:

$$y\left[l,k_t\right]=\sum_{p=0}^{P-1} h_p e^{-j\frac{2\pi l_p k_p}{MN}} x\left[\left[l-l_p\right]_M,\left[k-k_p\right]_N\right]+ v\left[l,k_t\right], t\in\{1,2\}, \tag{1}$$

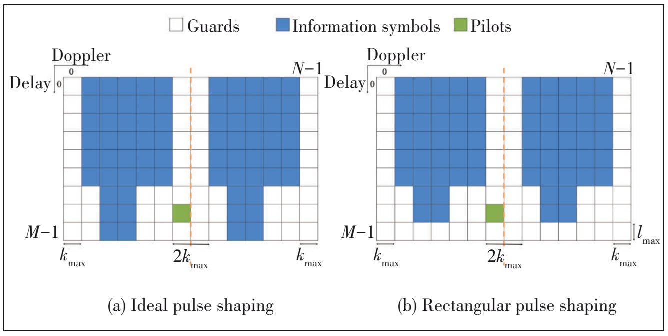

▲Figure 1. Ideal and rectangular pulse shaping

where $y[l,k_1]$ and $y[l,k_2]$ represent the received signal of the first and the second sub-frame, respectively; h_p denotes the channel response of the p-th path; l_p and k_p are the delay and Doppler indices of the p-th path. For the first sub-frame signal, since $k_1 \in \{0,1,...,\frac{N}{2}-1\}$, and $k_p \in \{-k_{max},...,0,1,...,k_{max}\}$, we can obtain $[k-k_p]_N \in [0,\frac{N}{2}-1+k_{max}] \cup [N-k_{max},N-1]$. From Eq. (1), we can see that the received signal of the first sub-frame is interfered by symbols of the second sub-frame when $[k-k_p]_N > \frac{N}{2}-1$. In order to avoid the interference with the first sub-frame, the guards are placed at the interference symbols in the second sub-frame, i.e., $x[l,k]=0, l=\{0,1,...,M-1\}, k \in \mathcal{G}_1$, where $\mathcal{G}_1 = \{[\frac{N}{2},\frac{N}{2}-1+k_{max}] \cup [N-k_{max},N-1]\}$. Moreover, interference symbols in the first frame are similar to the above analysis. Overall, the allocation of the information symbols can be obtained as $x[l,k], l=\{0,1,...,M-1\}, k \in \mathcal{G}_1 \cup \mathcal{G}_2$, where $\mathcal{G}_2 = \{[0,k_{max}-1] \cup [\frac{N}{2}-k_{max},\frac{N}{2}-1]\}$. Therefore, two sub-frames are not interfered with each other, and the equivalent channel of each sub-frame is identical. Furthermore, by considering the channel estimation in the delay-Doppler domain, pilots and guards should be carefully placed to protect the pilots from interference with other information symbols at the receiver. In order to utilize guard patterns introduced in this section, we allocate the pilots and the guards to the last $3l_{max}+2$ symbol positions along the delay domain. The allocation of the pilots and the corresponding guards for the i-th antenna is given by:

$$x_i[l,k]=\begin{cases} x_0, & k=k_0, l=M-il_{max}-1; \\ z^{k_0 l}, & k_0-2k_{max} \leqslant k \leqslant k_0+2k_{max}, M-il_{max}-1 \leqslant l \leqslant M-1, \end{cases} \tag{2}$$

where $k_0=\frac{N}{2}-1$ and $i \in \{1,2\}$.

Next, we introduce the transmit pattern. By deploying the Alamouti code structure, the transmit vectors at the first antenna and the second antenna are obtained as $\bar{\boldsymbol{x}}_1 = [\boldsymbol{x}_1^{\mathrm{T}}, \hat{\boldsymbol{x}}_2^{\mathrm{T}}]^{\mathrm{T}} \in \mathbb{C}^{NM}$ and $\bar{\boldsymbol{x}}_2 = [\boldsymbol{x}_2^{\mathrm{T}}, \hat{\boldsymbol{x}}_1^{\mathrm{T}}]^{\mathrm{T}} \in \mathbb{C}^{NM}$, where $\hat{\boldsymbol{x}}_1 = \boldsymbol{P}\boldsymbol{x}_1^*$, $\hat{\boldsymbol{x}}_2 = -\boldsymbol{P}\boldsymbol{x}_2^*$, and $\boldsymbol{P}$ is the permutation matrix. Then, the received signal can be obtained as

$$\boldsymbol{y}_1 = \boldsymbol{H}_1\boldsymbol{x}_1 + \boldsymbol{H}_2\boldsymbol{x}_2 + \boldsymbol{v}_1, \tag{3}$$

$$\boldsymbol{y}_2 = -\boldsymbol{H}_1\hat{\boldsymbol{x}}_2^* + \boldsymbol{H}_2\hat{\boldsymbol{x}}_1^* + \boldsymbol{v}_2, \tag{4}$$

where $\boldsymbol{y}_1$ and $\boldsymbol{y}_2$ are received signals at the first and the second sub-frame, respectively; $\boldsymbol{H}_1$ and $\boldsymbol{H}_2$ are the equivalent channels for the first and second sub-frame, respectively. From the block circulant property of $\boldsymbol{H}_1$ and $\boldsymbol{H}_2$, an alternative representation of Eqs. (3) and (4) are expressed as

$$\begin{bmatrix} \boldsymbol{y}_1 \\ \boldsymbol{y}_2 \end{bmatrix} = \begin{bmatrix} \boldsymbol{X}_1 & -\boldsymbol{X}_2^{\mathrm{H}} \\ \boldsymbol{X}_2 & \boldsymbol{X}_1^{\mathrm{H}} \end{bmatrix} \begin{bmatrix} \boldsymbol{h}_1 \\ \boldsymbol{h}_2 \end{bmatrix} + \begin{bmatrix} \boldsymbol{v}_1 \\ \boldsymbol{v}_2 \end{bmatrix}, \tag{5}$$

where $\boldsymbol{h}_1 \in \mathbb{C}^{MN/2}$ and $\boldsymbol{h}_2 \in \mathbb{C}^{MN/2}$ denote the first column of $\boldsymbol{H}_1$ and $\boldsymbol{H}_2$; $\boldsymbol{X}_1$ and $\boldsymbol{X}_2$ are the equivalent code words for the transmit vectors $\boldsymbol{x}_1$ and $\boldsymbol{x}_2$, respectively. By applying the maximal ratio combining receiver, the received signal of the two frames can be split apart as $\bar{\boldsymbol{y}}_1 = \bar{\boldsymbol{H}}\boldsymbol{x}_1 + \bar{\boldsymbol{v}}_1$ and $\bar{\boldsymbol{y}}_2 = \bar{\boldsymbol{H}}_e\boldsymbol{x}_2 + \bar{\boldsymbol{v}}_2$, where $\bar{\boldsymbol{H}} = \boldsymbol{H}_1^{\mathrm{H}}\boldsymbol{H}_1 + \boldsymbol{H}_2\boldsymbol{H}_2^{\mathrm{H}}$. Therefore, $\boldsymbol{x}_1$ and $\boldsymbol{x}_2$ are not interfered with each other, then the maximal likelihood (ML) detector or MMSE detector can be applied to decode $\boldsymbol{x}_1$ and $\boldsymbol{x}_2$, respectively. However, the computational complexity of the detectors is high since the non-linear iterations is involved in the ML receiver and the inverse operation of a high-dimensional matrix is applied in the MMSE receiver. By exploiting the matrix transformation and matrix decomposition, the computational complexity of the detector can be reduced to $O(l_{max}^2 MN^3)$, which is lower than the conventional MMSE receiver $O(M^3N^3)$.

2.2 Modified Approach with Rectangular Pulse Shaping

In this section, the transmission scheme in the rectangular pulse shaping is considered. We introduce the allocation of information symbols with the rectangular pulse shaping and design the corresponding transmitting and receiving structure.

The allocation of the information symbols is based on the input-output relation with rectangular pulse shaping, which is given by

$$\bar{y}\left[l,k_t\right] = \sum_{p=0}^{P-1} h_p e^{-j\frac{2\pi l_p k_p}{MN}} \alpha_p(l,k) x\left[\left[l-l_p\right]_M, \left[k-k_p\right]_N\right] + v\left[l,k_t\right], t \in \{1,2\}, \tag{6}$$

where

$$\alpha_p(l,k) = \begin{cases} e^{-j\frac{2\pi k}{N}} z^{k_p(l+M)}, & \text{if } l < l_p \\ z^{k_p l}, & \text{if } l \geqslant l_p. \end{cases} \tag{7}$$

Eq. (7) is the phase shift caused by the rectangular pulse shaping. The two sub-frames do not interfere with each other by allocating the guards introduced in Section 2.1. However, the equivalent channel of each sub-frame is different due to the phase shift. From Eq. (7), we can see that the phase shift of $x[l,k]$ is related to l,k when $l < l_p$ but only related to l when $l \geqslant l_p$. Then, the guards are placed at the last $l_{\max}$ symbols along the delay domain, i. e., $x[l,k] = 0, l = [M - l_{\max}, M-1], k \in \{0,1,...,N\}$ to keep the phase shift of each sub-frame identical. The allocation of information symbols, guards, and pilots in the OTFS frame is shown in Fig. 1. For the channel estimation, the position of pilots and guards is similar to that of the ideal pulse shaping in Eq. (2). Then, we also adopt the transmit code word of the Alamouti code structure in Section 2.1. However, the permutation matrix $\bar{\boldsymbol{P}}$ should be redesigned to keep the guards not being permuted. The transmit vectors at the first antenna and the second antenna are obtained as $\bar{\boldsymbol{x}}_1 = [\boldsymbol{x}_{11}^{\mathrm{T}}, \boldsymbol{x}_{12}^{\mathrm{T}}]^{\mathrm{T}} \in \mathbb{C}^{NM}$ and $\bar{\boldsymbol{x}}_2 = [\boldsymbol{x}_{21}^{\mathrm{T}}, \boldsymbol{x}_{22}^{\mathrm{T}}]^{\mathrm{T}} \in \mathbb{C}^{NM}$, respectively, where $\boldsymbol{x}_{12} = -\bar{\boldsymbol{P}}\boldsymbol{x}_{21}^{\ *}$ and $\boldsymbol{x}_{22} = -\bar{\boldsymbol{P}}\boldsymbol{x}_{21}^{\ *}$. Then, the received signal can be expressed as:

$$\begin{bmatrix}\bar{\boldsymbol{y}}_1\\ \hat{\boldsymbol{y}}_2^{\ *}\end{bmatrix} = \begin{bmatrix}\bar{\boldsymbol{H}}_1 & \bar{\boldsymbol{H}}_2\\ \boldsymbol{P}\bar{\boldsymbol{H}}_2^{\ *}\boldsymbol{P} & -\boldsymbol{P}\bar{\boldsymbol{H}}_1^{\ *}\boldsymbol{P}\end{bmatrix}\begin{bmatrix}\boldsymbol{x}_{11}\\ \boldsymbol{x}_{21}\end{bmatrix} + \begin{bmatrix}\boldsymbol{v}_1\\ \hat{\boldsymbol{v}}_2^{\ *}\end{bmatrix}, \qquad (8)$$

where $\hat{\boldsymbol{y}}_2 = \boldsymbol{P}\bar{\boldsymbol{y}}_2$; $\bar{\boldsymbol{y}}_1$ and $\bar{\boldsymbol{y}}_2$ are received signals of the first sub-frame and the second sub-frame, respectively; $\bar{\boldsymbol{H}}_1$ and $\bar{\boldsymbol{H}}_2$ are equivalent channels for $\boldsymbol{x}_{11}$ and $\boldsymbol{x}_{21}$, respectively. Then, the MMSE receiver or the MP receiver can be adopted to decode $\boldsymbol{x}_{11}$ and $\boldsymbol{x}_{21}$. In summary, the transmitting and receiving process with rectangular pulse shaping is shown in Fig. 2. Moreover, the proposed diversity scheme in this section can be extended to the multiple-antenna scenarios by employing the structure similar to Jafarkhani code, which is a quasi-orthogonal space-time block coding introduced in Ref. [19].

3 Closed-Loop System

In the closed-loop system, the transmitter dynamically varies the precoding matrix based on the CSI report such as the precoding matrix index, the rank indicator, and the channel quality indicator. However, the precoding problem in the closed-loop OTFS multiple-antenna system is not fully addressed. In this section, we observe the equivalence of the linear precoding between the delay-Doppler and the time-frequency domain. Then, delay-Doppler THP (DD-THP) schemes are introduced under the ZF or the MMSE criterion.

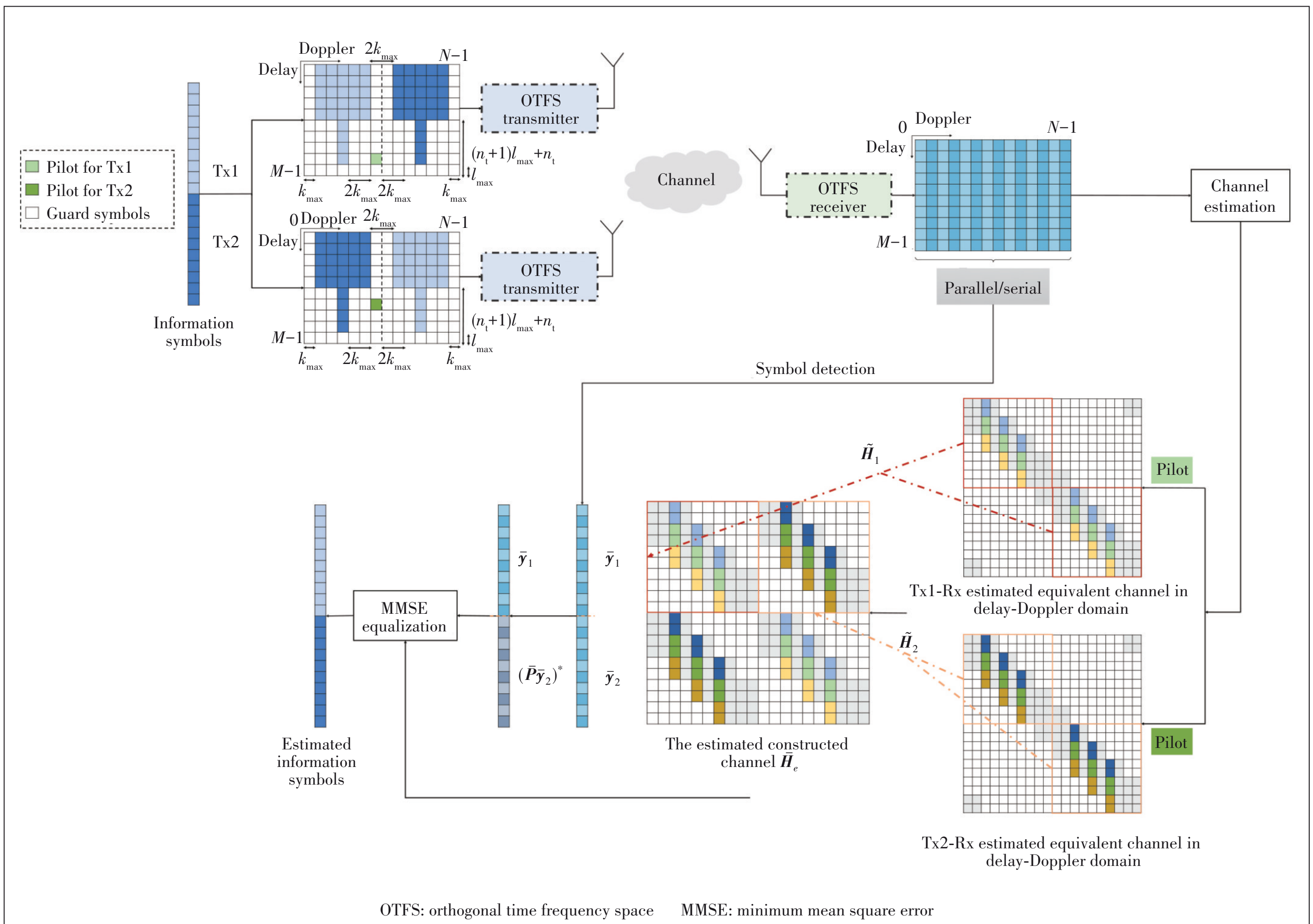

▲**Figure 2. Proposed diversity approach with rectangular pulse shaping**

Finally, we provide an overview of other closed-loop transmission schemes in the OTFS multiple-antenna systems.

3.1 Linear Precoding in Delay-Doppler Domain

In this section, the linear precoding in the time-frequency and the equivalent representation in the delay-Doppler domain are provided. We recall that in the MIMO-OFDM system, the linear codebook is selected to map symbols in the time-frequency domain to the transmit antennas. In contrast, symbols in the OTFS system are multiplexed in the delay-Doppler domain, then the precoding can be deployed in the delay-Doppler domain or the time-frequency domain. We observe that the precoding in the time-frequency domain can be alternatively represented in the delay-Doppler domain, which is shown as an example in the following. Considering a scenario that the transmitter is equipped with N_t antennas and the receiver is equipped with N_r antennas, we denote $\boldsymbol{W}_{TF} = \mathrm{diag}\{\boldsymbol{W}_1, \boldsymbol{W}_2, ..., \boldsymbol{W}_{MN}\}$ as the codebook in the time-frequency domain, where $\boldsymbol{W}_i, i = 1,2,...,MN$ is the codebook on each subcarrier. Then, the equivalent precoding in the delay-Doppler domain $\boldsymbol{W}_{DD}$ is given by

$$\boldsymbol{W}_{DD} = \left(\left(\boldsymbol{F}_N^* \otimes \boldsymbol{F}_M\right) \otimes \boldsymbol{I}_{N_t}\right)^{-1} \boldsymbol{W}_{TF}\left(\left(\boldsymbol{F}_N^* \otimes \boldsymbol{F}_M\right) \otimes \boldsymbol{I}_{N_t}\right), \tag{9}$$

where $\boldsymbol{F}_N$ and $\boldsymbol{F}_M$ are the discrete Fourier transform matrices with N-point and M-point, respectively; The operator $\otimes$ denotes the Kronecker product. By the equivalent representation in Eq. (9), the precoding process can be carried out in the delay-Doppler domain instead of the time-frequency domain since the channel estimation in the delay-Doppler domain is more stable than that in the time-frequency domain, especially in high-speed scenarios.

3.2 DD-THP Approach

THP is a well-known non-linear precoding scheme, which can also be adopted in the closed-loop OTFS multiple-antenna system. In this subsection, we introduce the DD-THP schemes in the delay-Doppler domain.

In the OTFS multiple-antenna system, the vector form of input-output relationship in the delay-Doppler domain is expressed as

$$\boldsymbol{y} = \boldsymbol{H}\boldsymbol{x} + \boldsymbol{v}, \tag{10}$$

where $\boldsymbol{H}$ is the equivalent channel matrix in the delay-Doppler domain; $\boldsymbol{x} \in \mathbb{C}^{N_t MN}$ is the vector form of the transmit symbols in the delay-Doppler domain; $\boldsymbol{y} \in \mathbb{C}^{N_r MN}$ is the received symbol in the delay-Doppler domain; $\boldsymbol{v} \in \mathbb{C}^{N_r MN}$ is the vector form of the zero mean circularly symmetric complex Gaussian noise at the receiver.

The equivalent channel matrix $\boldsymbol{H}$ is fed back to the transmitter for the precoding. A block diagram of applying THP in the OTFS multiple-antenna system is shown in Fig. 3. For the ZF-DD-THP approach, the conjugate transpose of the equivalent channel matrix $\boldsymbol{H}^H$ is decomposed into a unitary matrix and an upper triangular matrix, i.e., $\boldsymbol{H}^H = \boldsymbol{QR}$. Then, the forward and feedback filters are given by $\boldsymbol{F} = \boldsymbol{QG}$, $\boldsymbol{B} = \boldsymbol{R}^H\boldsymbol{G}$, respectively, where $\boldsymbol{G} = \mathrm{diag}\{r_1^{-1}, r_2^{-1}, ..., r_{N_r MN}^{-1}\}$ and $r_1, r_2, ..., r_{N_r MN}$ are the diagonal elements of $\boldsymbol{R}^H$. In addition, β is introduced to normalize the power of transmitted signals. The received signal is given by

$$\boldsymbol{y} = \boldsymbol{HFB}^{-1}(\boldsymbol{s} + \boldsymbol{a}) + \boldsymbol{v}. \tag{11}$$

Alternatively, the MMSE criterion can also be employed in the THP approach, which is called MMSE-DD-THP. We define

$$\bar{\boldsymbol{H}}_e = \boldsymbol{H}^{-1}\left(\boldsymbol{HH}^H + \frac{\sigma_n^2}{\sigma_v^2}\boldsymbol{I}\right). \tag{12}$$

Similarly, $\bar{\boldsymbol{H}}_e$ is decomposed into a unitary matrix and an upper triangular matrix, i.e., $\bar{\boldsymbol{H}}_e = \boldsymbol{QR}$. We can obtain $\boldsymbol{F} = \boldsymbol{QG}$ and $\boldsymbol{B} = \boldsymbol{R}^H\boldsymbol{G}$. Moreover, there are several approaches to further improvement of the MMSE-DD-THP. In Ref. [16], the authors rearranged the precoding order of symbols by considering the channel conditions. Furthermore, the linear Wiener transmit filter was adopted to obtain the optimizations after ordering the symbols[17]. In Ref. [18], a block-wise fashion and the Tx-Rx matrices were jointly optimized to minimize the MSE. However, it is noted that the computation complexity of DD-THP schemes is high due to the non-linear processing, which may limit the implementation of the DD-THP schemes in practice.

3.3 Other Precoding Approaches

The linear precoding is a widely used precoding technique in the cellular system. The advantage of the linear precoding over the THP is that the former has low computational complexity. The linear precoding is studied in the MIMO-OTFS system[14–16]. By exploiting the reciprocity of the uplink chan-

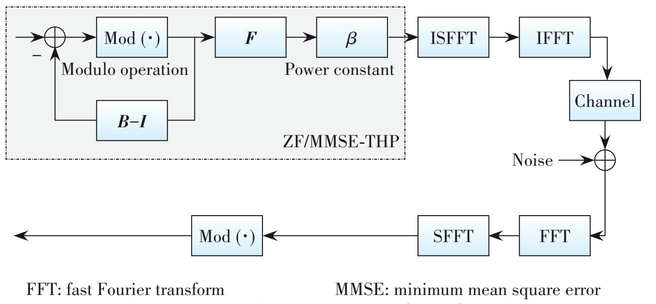

FFT: fast Fourier transform
IFFT: inverse fast Fourier transform
ISFFT: inverse symplectic finite Fourier transform
MMSE: minimum mean square error
OTFS: orthogonal time frequency space
THP: Tomlinson-Harashima precoding
ZF: zero-forcing

▲**Figure 3. Block diagram of applying THP in OTFS multiple-antenna system** nel and downlink channel, the authors in Ref. [14] proposed an uplink-aided transmission scheme in the MIMO-OTFS system. Since there are few scatterers between the transmitter and the user, and the angular spread of transmitted signals is small in the high-speed scenarios where the received signals occupy only a small part of the channel in the whole angle domain. The channel of the MIMO-OTFS system in the angle domain is sparse. By exploiting the reciprocity of wireless channels, the angle-delay-Doppler channel is estimated through the uplink channel estimation[15]. Then, based on the estimated angular direction of each user, each beamforming vector is formed to avoid multi-user interference in the downlink. In Ref. [16], an MRC precoder was proposed in the multi-user massive MIMO-OTFS system. The transmitter precodes the symbols by multiplying the Hermitian of the equivalent channels. Although the computational complexity of the precoding is low in Ref. [16], the interference among users is not completely eliminated, which degrades the BER performance.

4 Simulation Results

In this section, we evaluate the BER performance of the transmission schemes in the open-loop and the closed-loop MIMO-OTFS systems. The rectangular pulse shaping and the MMSE detector are employed in the simulation. The default setup of the simulation is listed in Table 1. We adopt the tapped-delay-line-A (TDL-A) channel model. The Doppler shift corresponding to the i-th tap is generated by Jakes' formula.

We evaluate the BER performance of our proposed open-loop scheme and the existing works in Fig. 4. We set the number of the receive antennas as one, and the number of the carriers is M = 32. In Fig. 4, the proposed diversity transmission scheme outperforms the Naive Tx Div. and the scheme in Ref. [12] at the speed of 500 km/h. The fundamental reason can be summarized into the two aspects: 1) the diversity gain and the coding gain can be obtained by using the proposed code word structure. That is the reason why the diversity scheme outperforms the Naive Tx Div. scheme; 2) The proposed scheme is achieved within one frame duration by precluding the two-frame block fading assumption. However, the scheme in Ref. [12] is implemented over the duration of the two consecutive frames where the channel state varies rapidly in the high-speed scenario, which leads to the poor BER performance. In comparison, the BER performance of the scheme in Ref. [12] becomes slightly better than the proposed scheme when the velocity reduces to 120 km/h. This is because: 1) the channel varies slowly at the speed of 120 km/h, which can be approximately regarded as the same; 2) the equivalent code word in Ref. [12] can achieve much coding gain since the orthogonality of the code word. In addition, the larger Doppler diversity can be achieved at the speed of 500 km/h over 120 km/h, which results in the better BER performance than that of 120 km/h.

In Fig. 5, we compare the BER performance of the ZF-DD-THP, the MMSE-DD-THP and the MMSE-THP with an ordering matrix. The number of the receive antennas is 2, and the

▼Table 1. Setup of simulation parameters

Parameters	Values
Number of OTFS symbols	14
Number of subcarriers	16, 64
Carrier frequency	4 GHz
Subcarrier spacing	15 KHz
Number of transmit antennas	2
Pulse shaping	Rectangular

OTFS: orthogonal time frequency space

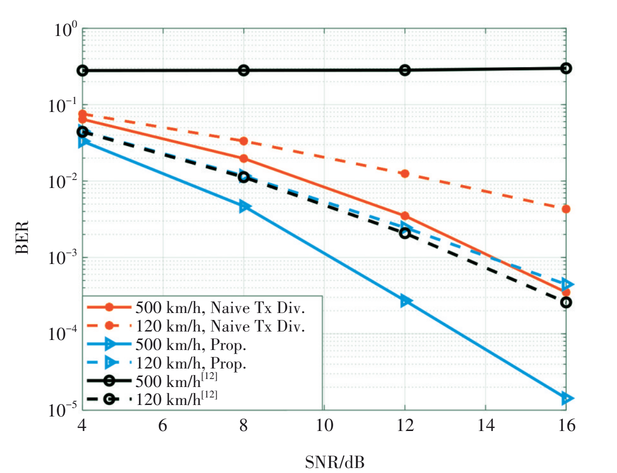

BER: bit error ratio
Naive Tx Div.: scheme that each antenna transmits the same symbols
Prop.: proposed diversity transmission scheme
SNR: signal-noise ratio

▲ Figure 4. Evaluated BER performance for diversity approaches in OTFS system

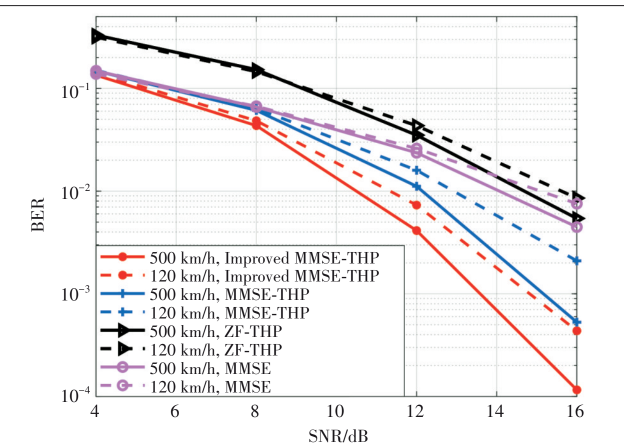

BER: bit error ratio
Improved MMSE-THP: scheme that considers the channel condition in MMSE-THP
MMSE: minimum mean square error
MMSE-THP: scheme that adopts THP by MMSE criteria
SNR: signal-noise ratio
THP: Tomlinson-Harashima precoding
ZF: zero-forcing

▲ Figure 5. Evaluated BER performance for the delay-Doppler (DD)-THP approaches in OTFS system

number of the carriers is set as M = 16. Benchmarks are shown as follows: 1) MMSE: each antenna transmits different symbols and uses MMSE equalization in the OTFS system; 2) ZF-THP: the transmission scheme based on ZF-DD-THP; 3) MMSE-THP: the transmission scheme based on MMSE-DD-THP; 4) Improved MMSE-THP: the transmission scheme based on the MMSE-THP considering the channel condition. We can see that compared with the ZF-DD-THP, the MMSE-DD-THP has a performance gain of about 4 – 5 dB at the same BER level. By considering the ordering matrix to encode the symbols in an optimized precoding order, the improved MMSE-THP can further improve the performance of MMSE-DD-THP.

5 Challenges and Opportunities

OTFS confronts many challenges when combined with the multiple-antenna system in the high-speed scenarios. In this section, we introduce challenges and opportunities in the open-loop and the closed-loop MIMO-OTFS transmission system.

5.1 Feedback in Closed-Loop Transmission

The equivalent channel with the dimension of $N_r MN \times N_t MN$ in the delay-Doppler domain is required to feed back to the transmitter in the DD-THP OTFS system, which causes a high-feedback overhead. Since the fast time-varying of the high-speed scenarios, the feedback of channel information may not match the current channel state, which results in the precoder mismatch to the current channel state. Therefore, how to reduce the feedback overhead and improve the real-time property of the precoder to match the current channel is inevitable in the closed-loop transmission systems. By observing the law of channel changes, one possible solution is to adopt a reliable channel prediction method by the previous channel estimation. Another approach is to design a codebook set to match the delay-Doppler channel, which is similar to the feedback pattern to OFDM closed-loop networks. In this way, the receiver selects a codebook to match the estimated channel and feeds back to the transmitter by a specific indicator. Then, each feedback become less.

5.2 Low-Complexity Precoding and Receiving Approaches

Due to the two-dimensional convolution in the delay-Doppler domain, the size of the precoding and the equalization matrices are large which results in the high computational complexity. Moreover, the linear receiver such as the MMSE receiver also leads to a high complexity due to the inverse operation of a high-dimensional matrix. Therefore, how to reduce the complexity of the precoding and equalization schemes is a big challenge in the OTFS multiple-antenna system. The study of the variational Bayes can be utilized to be the detector in the OTFS multiple-antenna systems.

5.3 Channel Estimation in MIMO-OTFS

The channel estimation with the fractional Doppler and the fractional delay is a more practical problem in the future research. Furthermore, in the aspect of the Doppler spectrum, most of the existing works focus on the channel estimation of the discrete-Doppler-spread (also known as limit-Doppler-spread) scenarios[20]. However, when the propagation environment involves many scattering objects, the Doppler shift of transmit paths are infinite and the Doppler spectrum is continuous, which is treated as the continuous-Doppler-spread channel. How to reduce the overhead of the channel estimation in the meantime improve the accuracy in these practical channel models is a big challenge. In Ref. [21], a low-dimensional subspace is constructed to characterize the variation of the equivalent channel responses in the continuous-Doppler-spread channel, which is modeled by a sum of the projection coefficients and the basis functions.

6 Conclusions

In this paper, we introduce both the open-loop and the closed-loop multi-antenna approaches for the OTFS with the ideal and the rectangular pulse shaping. In the open-loop design, the main contribution is that the transmit diversity approaches resembling space-time coding are provided, which take the practical issues into account, i. e., the rectangular pulse shaping and the rapidly time-varying channel. For the closed-loop design, we suggest to adopt the Tomlinson-Harashima precoding in the delay-Doppler domain since we have developed the relation between the precoding matrix in the time-frequency domain and that in the delay-Doppler domain. The reason why we recommend precoding in the delay-Doppler domain is that the channel in the delay-Doppler domain varies more slowly within a frame in contrast to that in the time-frequency domain. In the end, we discuss challenges and opportunities of the OTFS multiple-antenna system, which can be further investigated in future.

References

[1] LI S Y, YUAN W J, WEI Z Q, et al. A tutorial to orthogonal time frequency space modulation for future wireless communications [C]//2021 IEEE/CIC International Conference on Communications in China (ICCC Workshops). Xiamen, China, 2021: 439 – 443. DOI: 10.1109/ICCCWorkshops52231.2021.9538891
[2] WEI Z Q, YUAN W J, LI S Y, et al. Orthogonal time-frequency space modulation: a promising next-generation waveform [J]. IEEE wireless communications. 2021, 4(28): 136 – 144. DOI: 10.1109/MWC.001.2000408
[3] RAVITEJA P, PHAN K T, HONG Y, et al. Interference cancellation and iterative detection for orthogonal time frequency space modulation [J]. IEEE transactions on wireless communications, 2018, 17(10): 6501 – 6515. DOI: 10.1109/TWC.2018.2860011
[4] LI S Y, YUAN W J, Wei Z Q, et al. Cross domain iterative detection for orthogonal time frequency space modulation [J]. IEEE transactions on wireless communications. 2021. DOI: 10.1109/TWC.2021.3110125

[5] QU H Y, LIU G H, ZHANG L, et al. Low-complexity symbol detection and interference cancellation for OTFS system [J]. IEEE transactions on communications, 2021, 69(3): 1524 – 1537. DOI: 10.1109/TCOMM.2020.3043007
[6] SURABHI G D, CHOCKALINGAM A. Low-complexity linear equalization for 2 × 2 MIMO-OTFS signals [C]//IEEE 21st International Workshop on Signal Processing Advances in Wireless Communications. Atlanta, USA: IEEE, 2020: 1 – 5. DOI: 10.1109/SPAWC48557.2020.9154292
[7] SINGH P, MISHRA H B, BUDHIRAJA R. Low-complexity linear MIMO-OTFS receivers [C]//IEEE International Conference on Communications Workshops. Montreal, Canada: IEEE, 2021: 1 – 6. DOI: 10.1109/ICCWorkshops50388.2021.9473839
[8] VUCETIC B, YUAN J H. Space-time coding [M]. Chichester, UK: John Wiley & Sons, 2003. DOI: 10.1002/047001413x
[9] ALAMOUTI S M. A simple transmit diversity technique for wireless communications [J]. IEEE journal on selected areas in communications, 1998, 16(8): 1451 – 1458. DOI: 10.1109/49.730453
[10] TAROKH V, SESHADRI N, CALDERBANK A R. Space-time codes for high data rate wireless communication: Performance criterion and code construction [J]. IEEE transactions on information theory, 1998, 44(2): 744 – 765. DOI: 10.1109/18.661517
[11] BOMFIN R, CHAFII M, NIMR A, et al. Channel estimation for MIMO space time coded OTFS under doubly selective channels [C]//2021 IEEE International Conference on Communications Workshops. Montreal, Canada: IEEE, 2021: 1 – 6. DOI: 10.1109/ICCWorkshops50388.2021.9473618
[12] AUGUSTINE R M, SURABHI G D, CHOCKALINGAM A. Space-time coded OTFS modulation in high-Doppler channels [C]//IEEE 89th Vehicular Technology Conference. Kuala Lumpur, Malaysia: IEEE, 2019: 1 – 6. DOI: 10.1109/VTCSpring.2019.8746394
[13] DELFELD J, RAKIB S S. Tomlinson-harashima precoding in an OTFS communication system: US11018731 [P]. 2021
[14] LIU Y, ZHANG S, GAO F F, et al. Uplink-aided high mobility downlink channel estimation over massive MIMO-OTFS system [EB/OL]. (2020-03-16) [2021-09-18]. https:// arxiv.org/abs/2003.07045
[15] LI M Y, ZHANG S, GAO F F, et al. A new path division multiple access for the massive MIMO-OTFS networks [J]. IEEE journal on selected areas in communications, 2021, 39(4): 903 – 918. DOI: 10.1109/JSAC.2020.3018826
[16] PANDEY B C, MOHAMMED S K, RAVITEJA P, et al. Low complexity precoding and detection in multi-user massive MIMO OTFS downlink [J]. IEEE transactions on vehicular technology, 2021, 70(5): 4389 – 4405. DOI: 10.1109/TVT.2021.3061694
[17] HABENDORF R, IRMER R, RAVE W, et al. Nonlinear multiuser precoding for non-connected decision regions [C]//IEEE Workshop on Signal Processing Advances in Wireless Communications. New York, USA: IEEE, 2005., 535 – 539, DOI: 10.1109/SPAWC.2005.1506197
[18] KUSUME K, JOHAM M, UTSCHICK W, et al. Efficient Tomlinson-Harashima precoding for spatial multiplexing on flat MIMO channel [C]//IEEE International Conference on Communication. Seoul, Korea (South): IEEE, 2005: 2021 – 2025. DOI: 10.1109/ICC.2005.1494693
[19] JAFARKHANI H. A quasi-orthogonal space-time block code [J]. IEEE transactions on communications, 2001, 1(49): 1 – 4, DOI: 10.1109/26.898239
[20] QU H Y, LIU G H, ZHANG L, et al. Low-dimensional subspace estimation of continuous-Doppler-spread channel in OTFS systems [J]. IEEE transactions on communications, 2021, 69(7): 4717 – 4731. DOI: 10.1109/TCOMM.2021.3072744
[21] RAVITEJA P, PHAN K T, HONG Y. Embedded pilot-aided channel estimation for OTFS in delay – Doppler channels [J]. IEEE transactions on vehicular technology, 2019, 68(5): 4906 – 4917. DOI: 10.1109/TVT.2019.2906357

Biographies

WANG Dong received the B.Eng. degree from the School of Electronic and Information Engineering, Hebei University, China in 2016. He is currently pursuing the Ph.D. degree with the State Key Laboratory of Rail Traffic Control and Safety, Beijing Jiaotong University, China. His current research interests include multiway relaying communications and MIMO communications.

WANG Fanggang (wangfg@bjtu.edu.cn) received the B.Eng. and Ph.D. degrees from the School of Information and Communication Engineering, Beijing University of Posts and Telecommunications, China in 2005 and 2010, respectively. He was a Post-Doctoral Fellow with the Institute of Network Coding, The Chinese University of Hong Kong, China from 2010 to 2012. He was a visiting scholar with the Massachusetts Institute of Technology, USA from 2015 to 2016 and the Singapore University of Technology and Design, Singapore in 2014. He is currently a professor with the State Key Laboratory of Rail Traffic Control and Safety, School of Electronic and Information Engineering, Beijing Jiaotong University, China. His research interests are in wireless communications, signal processing, and information theory. He served as an editor for the *IEEE Communications Letters* and a technical program committee member for several conferences.

LI Xiran received the B.Eng degree from the school of Information and Communication Engineering, Beijing Jiaotong University, China in 2021. She is currently pursuing the M.A. degree with the State Key Laboratory of Rail Traffic Control and Safety, Beijing Jiaotong University. Her current research interests include MIMO communications and orthogonal time frequency space.

YUAN Pu received the B.Eng. degree from Tianjin University, China in 2007 and the M.S. and Ph.D. degrees from Nanyang Technological University, Singapore in 2010 and 2015, respectively. He is currently with vivo Mobile Communication Co., Ltd., China. From 2016 to 2019, he was a research engineer with the 2012 Laboratories, Huawei Technologies Company, Ltd., China. His research interests include signal processing in communication and information theory.

JIANG Dajie received the B.S. degree in communication engineering and M.S. degree in digital signal processing from Beijing University of Posts and Telecommunications, China in 2005 and 2008, respectively. From 2008 to 2017, he was a research engineer for 4G and 5G wireless research & standardization with China Mobile Research Institute. He is currently with vivo Mobile Communication Co., Ltd., China. His research interests include potential technologies for 6G including RIS and joint communication and sensing.